

Innovative Techniques For Two-Phase Flow Measurements

Wael H. Ahmed* and Basel I. Ismail**

*Component Life Technology, Atomic Energy of Canada Ltd., Canada, **Department of Mechanical Engineering, Lakehead University, Canada

Received: November 5, 2007; Accepted: November 27, 2007; Revised: November 30, 2007

Abstract: Two-phase flow is important in an increasing number of applications and industries. For example, the safety analysis codes for the nuclear energy industry require closure relations for the vapor-liquid interfacial transfer terms, while accurate two-phase pressure drop models are necessary to design the piping systems in the oil and gas industry. Also, two-phase flow occurs in heat exchangers, steam generators, chemical reactors, oil transportation and many other process equipments. In addition, development of accurate and suitable instrumentations for on-line monitoring and measurement of the solids concentration and velocity in gas-solid two-phase flows has proven to be a challenging problem with many scientists and engineers worldwide developing novel techniques for this application. This paper presents a review on the electrical-based measurement techniques for gas-solid and gas-liquid two-phase flows along with the most recent patents developed for two-phase flow measurements. Also, development of a novel method for the design of capacitance sensors for void fraction measurement and flow pattern identification was presented in detail.

Keywords: Two-phase flow, gas-solid flow, gas-liquid flow, novel design method, capacitance sensor, recent patents, void fraction.

1. INTRODUCTION

Online, continuous, two-phase flow measurement is often necessary, particularly in the oil and gas, nuclear energy and chemical processing industries. Reliable measurements of the void fraction and flow pattern identification are important for accurate modeling of two-phase systems. Void fraction can be measured using a number of techniques, including radiation attenuation (X or γ -ray or neutron beams) for line or area averaged values, optical or electrical contact probes for local void fraction, impedance technique using capacitance sensors and direct volume measurement using quick-closing valves. The use of the different techniques depends on the applications, and whether a volumetric average or a local void fraction measurement is desired. The radiation attenuation method can be expensive and from a safety aspect difficult to implement, while intrusive probes disturb the flow field. On the other hand, the impedance measurement technique is practical and cost-effective method for void fraction measurement. The technique is non-intrusive and relatively simple to design and implement. Impedance or capacitance sensors have been used successfully to measure time and volume averaged void fraction, and its instantaneous output signal has been used to identify the flow pattern [1]. In this paper, electrical-based techniques for gas-liquid and gas-solid flows measurements are reviewed. The paper is divided into two parts: In the first part, gas-solid flow measurements with their important and relevant application to pneumatic conveying systems are discussed. However, the detailed description of different techniques cannot be covered exhaustively here. Therefore, detailed consideration is focused on the development of a novel method for the design of a capacitance sensor used in

gas-liquid two-phase flow measurements in the second part of the paper.

2. RECENT DEVELOPMENTS IN TWO-PHASE FLOW MEASUREMENTS

2.1. Gas-Solid Two-Phase Flows

Gas-solid Two-phase flows, particularly those solids in the forms of powder and grain transported in gases (typically air) through a pipeline, are important in pneumatic conveying which has widespread applications across many industries including chemical, food processing, cement, mining, petrochemical, pharmaceutical, semiconductor, and in transporting pulverized coal in fuel lines of thermal power plants. Moving fluidized-beds may also be regarded as a form of gas-solid flows. This wide application has led to extensive research on gas-solid two-phase flow systems.

Gas-solid flows (also known as particulate flows), such as those in pneumatic conveying systems, are usually classified as dilute- or dense-phase flow. The dilute-phase flow can be normally achieved with low concentrations of solids (typically below 10%) and the simultaneous condition of high gas velocities in the gas-solid flow mixture [2]. In the dilute-phase conveying, the solid particles are fully dispersed or suspended in the flow and no deposition occurs. The velocity at which solids are traveling in a dilute-phase conveying is important. If they are traveling too slowly, solids can drop out from the flowing suspension and pipe blockage can occur. If they are traveling too quickly this can lead to unnecessarily high pipeline wear and power consumption due to system pressure drop [3]. Flow patterns in a dense pneumatic conveying system, however, show many interesting features and analogies with gas-liquid flows, such as slug, plug, and stratified flow regimes [4]. Dense-phase flow in pneumatic conveying systems have the relative benefits of a low air requirement and hence energy demand, low pipeline erosion and low product degradation

*Address correspondence to this author at the Component Life Technology, Atomic Energy of Canada Ltd., Canada; Tel: +1(613) 584-8811; Fax: +1(613) 584-8031; E-mail: ahmedw@aecl.ca

[5]. However, dense-phase pneumatic conveying may lead to unstable flows, caused by insufficient air velocity, and deposition. These unstable flows and deposition often cause pipe blockage and vibration that can be extremely difficult to remedy.

The fundamental system components of a conventional pneumatic conveying system are: an air mover, a feeder for the solids material to be conveyed, the conveying pipeline, and a receiver to disengage the conveyed solids and carrier gas (typically air). Local solids concentration and velocity are two of the most important parameters characterizing gas-solid flows. Development of accurate and suitable instrumentations for on-line monitoring and measurement of the solids concentration and velocity in gas-solid two-phase flows has proven to be a challenging task with many scientists and engineers worldwide developing novel techniques for this application. This is particularly due to spatial and temporal fluctuations of both the solids concentration and velocity during the pneumatic transportation [6]. The results of these measurements can be used to ensure efficient and economic pneumatic conveying operation, prevent blockage and hazardous damages and maintain safety standards. This paper presents a review on a range of existing and recent techniques used to measure solids concentration and velocity in gas-solid flows, such as those widely used in pneumatic conveying systems.

2.2. Measurement Techniques for Gas-Solid Flow Systems

The measurements and visualization of gas-solid flows, such as those involved in pneumatic conveying systems, could be performed using a range of noninvasive and non-intrusive electrical impedance, optical transmission [7], radiography and radiometric sensing [8], and other measurement techniques. The application of capacitance sensors for measuring local solids concentrations in a gas-solid flow was established decades ago [9, 10]. Chang *et al.* [11] tested strip- or ring-type capacitance transducers that could be used in non-electrically conductive (dielectric) pipes to non-destructively detect powder flow or measure powder thickness using the dielectric constant difference of the gas and powder. Capacitance impedance rings are noninvasive, simple and relatively inexpensive for implementation and provide high temporal resolution. However, those devices are difficult to calibrate and care must be taken when using correlation models for different gas-solid flow patterns to convert electrical impedance to solid concentrations [12]. In a dense-phase pneumatic conveying where density gradient exists in the gas-solid flow caused by a non-uniform distribution of solids in a pipe cross section, electrical capacitance tomography (ECT) can be effectively used [4; 5; 13]. In an electrical process tomography, the capacitance-sensing electrodes are installed at equal intervals around the periphery of the pipe, in order to obtain the three-dimensional distribution of solids along the direction of the gas-solid flow. The electrodes are usually installed in a noninvasive way, i.e. outside the pipe made of dielectric material [14]. The process tomography or tomographic imaging technique has the potential of producing cross-sectional images of the distribution of flow components in a conveying pipeline from which solids velocity and

concentration profiles of a section of a pipeline can be obtained. Brown *et al.* [15] developed a tomographic technique for imaging gas-solid flow distributions in pneumatic conveying pipelines. Their technique utilized ultrasonic transmission-mode measurements constrained to the megahertz region. They performed image reconstruction using a back-projection method implemented with standard graphics algorithms. Brown *et al.* [15] applied their technique to simulate reconstructions of dense and dilute distributions and obtained results demonstrating the capabilities and limitations of their technique. They also addressed aspects of transducer array design. Recently, Steiner *et al.* [16] proposed a dual-mode ultrasound and electrical capacitance process tomography sensor for measurements of gas-solid flow. In their method, the ultrasound image is used as a priori information for the finite element method-based capacitance reconstruction algorithm. They [16] reported that a significant improvement in image quality can be achieved with the proposed dual-mode tomography process sensor.

Jiang and Xiong [17] introduced a novel noninvasive electrostatic method for measurement of the solids velocity and mass flow rate in gas-solid flow. In their system, the measurement of the velocity and mass flow rate were realized by an electrostatic sensor capable of detecting the electrostatic signals of solid powder in the gas-solid flow. The transit time of powder was measured by cross-correlating electrostatic signals, and the velocity was calculated. By correlating the voltage on electrostatic sensor and the fixed mass flow rate, the voltage-mass flow rate curve of the sensing system was established. Jiang and Xiong [17] concluded that electrostatic method can be used to trace and measure the velocity of the solid phase, and the method is capable of performing on-line measurements of the mass flow rate of the gas-solid flow.

3. CAPACITANCE SENSORS FOR GAS-LIQUID TWO-PHASE FLOWS

The principle of the capacitance method is based on the differences in the dielectric constants of the two phases in the flow, and the capacitance measured across the sensors is dependent on the volume ratio of the two phases. There are, however, several disadvantages of the impedance technique, which are sometimes difficult to resolve. For example, the capacitance measurement is sensitive to the void fraction distribution or flow regimes due to the non-uniformity of the electrical field inside the measuring volume. This, however, can be compensated by first identifying the flow pattern. The measurement is also sensitive to the changes in electrical properties of the two phases due to temperature. The noise due to the electromagnetic field around the sensor and connecting wires can significantly affect the signal and needs to be minimized through proper design of the sensor shield. The sensitivity of the capacitance meter is also improved by Andrade [18]. He used a full power supply potential swing on the shield electrodes to allow for the use of simpler shield electrode design. Using the full swing improves the capacitance background and balances such noises as the wire capacitances. Furthermore, it is difficult to resolve the change in phase distribution within the sensor measurement volume. The sensitivity to the flow pattern can be increased through better design of the sensors. For example, Hung *et*

al. [19] used eight electrodes along the circumference of the tube to obtain a tomographic image of the two-phases. On the other hand, homogenizing the electric field in the axial direction minimizes the error due to the void distribution in the measuring volume. This could be done by using rotating type sensors as suggested by Merilo *et al.* [20] and Lucas and Simonian [21] or by using helical electrodes as discussed by Geraets and Borst [22] and Kenneth and Rezkallah [23]. The electrical capacitance tomography technique was also implemented recently by Gamio *et al.* [24] to image various two-phase gas-oil horizontal flows in a pressurized pipeline. They emphasized the potential of this technique for real-time flow visualization and flow regime identification in practical industrial application at high pressure operating conditions. Electrical Impedance Tomography (EIT) is also introduced in a recent patent by Wang [25] as a new signal processing method. The method is used on-line to obtain accurate estimates of the local disperse phase volumetric flow rate, the mean disperse and continuous phase volume fractions and the distributions of the local axial, radial and angular velocity components of the disperse phase.

Several different configurations of capacitance sensors, including flat plate, concave, ring, helical and multiple helical wound in contact or isolated from the fluid, have been widely investigated [23, 26-29]. However, there are fewer studies on the optimization of the design to obtain good signal to noise ratio and high sensitivity to the different flow patterns. Elkow and Rezkallah [23] compared the performance of concave and helical type sensors and determined that the problems associated with helical type sensors, including the nonlinear response, poor sensitivity and poor shielding, can be eliminated by using the concave type sensors. The accuracy of the concave parallel sensors can be improved by having both electrodes of equal length to decrease the non-uniformity of the electric field between the two electrodes and eliminate the non-linear response. Based on several tests, they also recommended that the distance between the electrodes and the shield should be large relative to the separation distance between the two electrodes in order to improve the immunity to stray capacitance.

In this paper, a systematic method for the design of capacitance sensors for void fraction measurement and flow pattern identification is presented. Two different configurations of the sensors are considered: concave and ring type Fig. (1). For the ring types sensor each electrode covers the entire circumference, except for a small gap to facilitate the installation of the sensor around the tubes, and are separated in the axial direction of the tube Fig. (1a), while in the concave sensor, two brass strips are mounted on the tube circumference opposite to each other Fig. (1b). The difference in the electrode geometry results in different electric fields within the measurement volume and hence in the sensitivity and response of the sensors. The two geometries are analyzed for the signal to noise ratio and the sensitivity to the void fraction and flow pattern. Experiments were performed to validate the design theory and to evaluate the sensor characteristics in actual operating conditions using air-oil two-phase flow in a horizontal pipe. To more objectively identify the flow pattern, the probability density function (PDF) and power spectral density (PSD) of the time trace of the void fraction signal is analyzed in a similar manner to that done by Jones and Zuber [30].

4. CAPACITANCE SENSOR DESIGN

The capacitance sensors need to be designed for accurate measurement of the void fraction, and have sufficient time response to detect the variations for the different flow patterns. The value of the capacitance across the sensors is related to the phase distribution and dielectric properties of the two-phases. The relationship between the capacitance and the void fraction is dependent on the dielectric values of the two phases, cross-sectional area of the sensors, and the separation distance between the two electrodes. A dielectric material placed between two conductor plates acts as an insulator to increase the charge storage capabilities because the dielectric contains charged molecules that are randomly oriented. When an external field is applied across the two plates, the charged molecules align themselves with the electric field and produces dipoles, where the positive charges of each molecule are in the direction of the applied field and the negative charges oppose the field. An internal

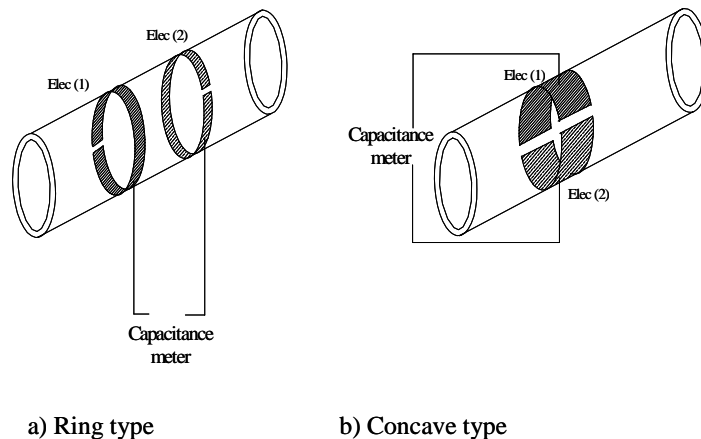


Fig. (1). Schematic of electrodes configurations.

electric field, opposite in direction of the external electric field, will result with a consequent reduction of the overall electric field and the overall potential. It is important to understand the theory of the capacitance sensor technique to properly optimize the sensor design. For simplicity, this can be illustrated using a simple parallel plate capacitor to show the effect of a dielectric material on the capacitance. Neglecting edge effects, the uniform electric field between the two plates of the capacitor in vacuum space without the dielectric medium, with charge density ρ_f and the permittivity of free space, $\epsilon_o = 8.854 \times 10^{-12} \text{C}^2 \text{N}^{-1} \text{m}^{-2}$, can be written as:

$$E = \frac{\rho_f}{\epsilon_o} \quad (1)$$

When a dielectric material is inserted to fill the entire space between the plates, the dielectric is polarized, and a polarization charge of density ρ_p appears on the two surfaces. For a uniform electric field out from a plane, the electric field can be written as:

$$E = \frac{(\rho_f + \rho_p)}{\epsilon_o} \quad (2)$$

The polarized charge density is:

$$\rho_p = \epsilon_o \chi E \quad (3)$$

where χ is the electric susceptibility of the material. Finally we can write the capacitance as:

$$C = \frac{\epsilon_o (1 - \chi) A}{d} \quad (4)$$

and the dielectric constant κ is defined as:

$$\kappa = (1 - \chi) \quad (5)$$

The permittivity ϵ is sometimes used to characterize the dielectric behavior of the matter and is related to the permittivity of the free space as

$$\epsilon = \epsilon_o \cdot \kappa \quad (6)$$

In order to mathematically represent the output signal as a function of the void fraction, the capacitance measured by a transducer for two-phase flow can be treated as an approximation of a parallel or series combination of capacitors with different dielectric constants. In this work, the performance of two different types of sensor configurations is investigated, and a design method to optimize the sensor performance is developed. The sensor output is sensitive to the flow pattern and to incorporate the flow pattern in the theoretical analysis, it is important to clearly classify the flow patterns. To minimize the number of flow patterns, only the basic flow patterns are considered here. For horizontal pipes: bubbly, stratified, slug, and annular flow are used and for vertical pipes: bubbly, slug, and annular are considered. Churn flow is difficult to simulate in our analysis.

4.1. Ring Type Sensors

If we consider only stratified, annular and long slug flow patterns among the basic flow patterns listed before, the electric field between two ring electrodes in free space can be schematically presented in Fig. (2a). Assuming the electrical field is shielded outside the tube and neglecting the radial electric field, the distribution can be approximated to that shown in Fig. (2b). Therefore the electric field can be assumed approximately constant in the axial direction and the two rings equivalent to parallel flat disks. The equivalent capacitance circuit method can be used to analyze this problem [11]. In this method, the two phases are modelled as series or parallel capacitors between the electrodes. This equivalent circuit is based on the distribution of the two phases inside the channel and is illustrated in Fig. (3). By considering the two electrodes as two imaginary disks in parallel with a separation distance (d), the two phases distributed horizontally will be equivalent to two capacitances in series Fig. (3a), while the two phases distributed in the vertical direction will be equivalent to two parallel capacitances Fig. (3b). The equivalent circuits for different two-phase distributions are shown Fig. (4a) through d as discussed by Chang *et al.* [11]. The theoretical output

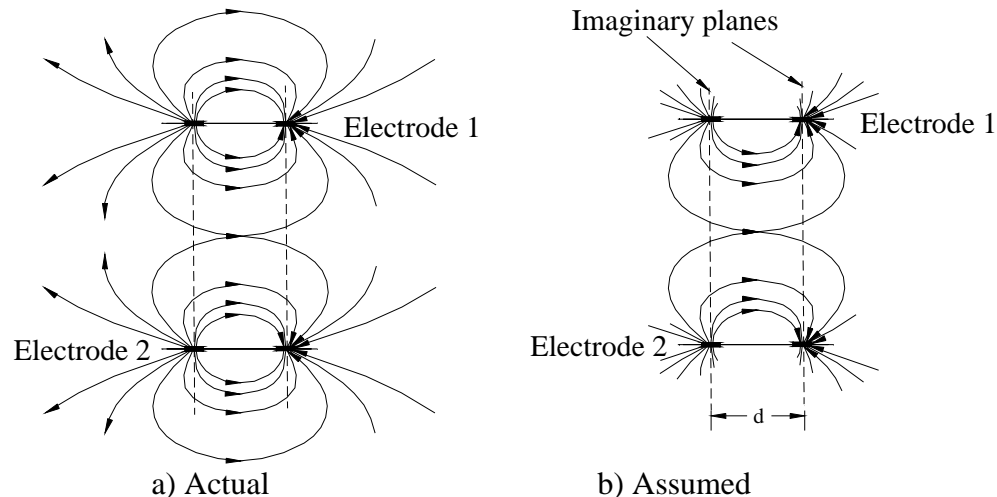


Fig. (2). Schematic of electrical field profile generated by two ring electrodes.

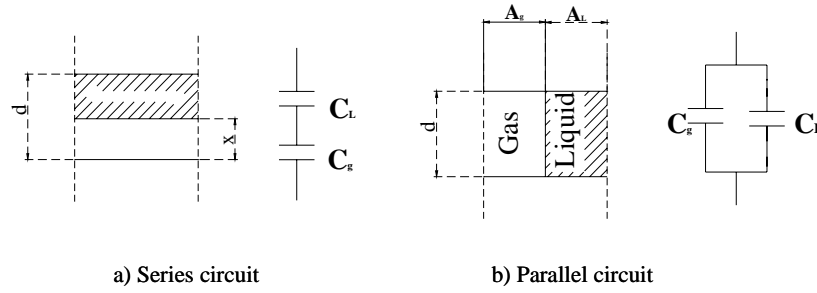


Fig. (3). Capacitance circuit equivalent to two-phase flow distribution.

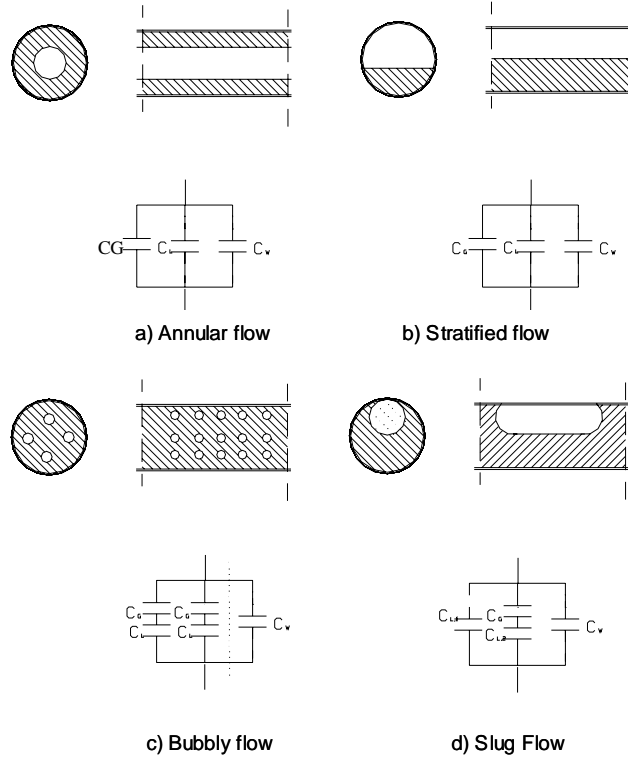


Fig. (4). Equivalent capacitance circuits for typical flow regimes (Adapted from Chang *et al.* [11]).

capacitance as a function of void fraction for annular, stratified and long slug flow can be obtained by considering the equivalent circuit method represented in Fig. (4a & b), and the total equivalent capacitance for both circuits can be calculated as:

$$C_T = C_g + C_L + C_w \tag{7}$$

For annular or stratified flow

$$C_T = \frac{K_g \epsilon_0 A_g}{d} + \frac{K_L \epsilon_0 A_L}{d} + \frac{K_w \epsilon_0 A_w}{d} \tag{8}$$

$$C_T = \frac{K_g \epsilon_0 A_g}{d} + \frac{K_L \epsilon_0 (1 - A_g)}{d} + \frac{K_w \epsilon_0 \times \frac{\pi}{4} ((D+t)^2 - D^2)}{d} \tag{9}$$

The void fraction is defined as

$$\alpha = \frac{V_G}{V_T} = \frac{A_G \cdot d}{A_T \cdot d} = \frac{A_G}{A_T} \tag{10}$$

where V_G and V_T are the volume of gas and total volume respectively.

By dividing equation (9) by the cross-sectional area of the pipe results in

$$C_T = \frac{\pi D^2 \times \epsilon_0}{4d} \left[K_g \alpha + K_L (1 - \alpha) + K_w \left(\left(1 + \frac{t}{D} \right)^2 - 1 \right) \right] \tag{11}$$

where, t is the pipe wall thickness and κ_w is the dielectric constant of the pipe material.

4.2. Concave Type Sensors

A similar analogy is used for the concave type sensors, however, an equivalent geometrical shape is introduced (Fig. 5a through c), where the change of the electrical field due to the curvature of the electrode is neglected [26]. Then, the total capacitance for stratified or annular flow pattern can be written as:

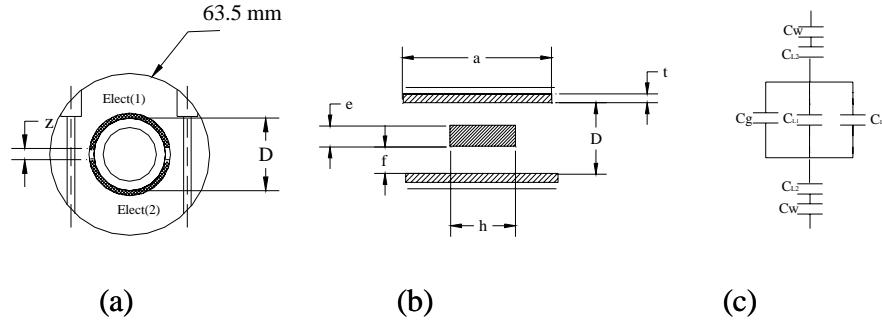


Fig. (5). (a),(b) Geometrical simplification of the concave type capacitance sensor, (c) Equivalent capacitance circuits for annular and core flow regimes.

$$C_T = \left(\frac{1}{C_w} + \frac{1}{C_{L2}} + \frac{1}{C_g + C_{L1} + C_{L1}} + \frac{1}{C_w} + \frac{1}{C_{L2}} \right) \quad (12)$$

The equivalent geometrical parameters can be defined as

$$d = \sqrt{\alpha} \cdot (D - 2 \cdot t) \quad e = d = \sqrt{\alpha} \cdot (D - 2 \cdot t)$$

$$f = \frac{1}{2} (D - \sqrt{\alpha} \cdot (D - 2 \cdot t)) \quad a = \frac{1}{2} (\pi D - 2 \cdot z) \quad (13)$$

Based on the two phases distribution shown in Fig. (5), and using the capacitance circuit analogy, the capacitances in equation (12) can be written as:

$$C_w = \kappa_w \epsilon_o \frac{a \times L}{t} \quad C_g = \kappa_g \epsilon_o \frac{h \times L}{e}$$

$$C_{L1} = \kappa_L \epsilon_o \frac{a \times L}{e} \quad C_{L2} = \kappa_L \epsilon_o \frac{a \times L}{f} \quad (14)$$

The above analysis may be used to estimate the capacitance of such a sensor by substituting the permittivity of the free space and the dielectric constant of the liquid as well as the geometrical parameters listed in equation (13) as a function of the void fraction. The set of equations (12) to (14) relate the capacitance to the void fraction and can be used to investigate the sensitivity and/or to compare different designs.

4.3. Design Method Applied to Different Flow Patterns

Although the theoretical model discussed above considered only stratified and annular flow, the analysis could be

extended to other flow patterns in order to design and optimize the capacitance sensor. As an example, plug flow is considered, and in particular the case where an elongated bubble with a length l_G in a horizontal pipe is passing through a pair of ring type sensors as shown in Fig. (6a). The bubble can be assumed as a horizontal cylinder with cross sectional area A_G and occupying a length l between the two electrodes. Assuming a constant electric field between the electrodes, the equivalent capacitance circuit using the same analogy as before is shown in Fig. (6). In this case

$$C_T = \frac{C_g + C_{L1}}{C_g C_{L1}} + C_{L2} + C_w \quad (15)$$

and the volumetric void fraction is different from the cross sectional void fraction and can be calculated as

$$\alpha = \frac{V_G}{V_T} = \frac{A_G \cdot l_G}{A_T \cdot d} \quad (16)$$

The capacitances in equation (15) can be written as

$$C_w = \frac{\kappa_w \epsilon_o \frac{\pi}{4} ((D+t)^2 - D^2)}{d} \quad C_{L1} = \frac{\kappa_L \epsilon_o A_g}{d-l}$$

$$C_{L2} = \frac{\kappa_L \epsilon_o (A_t - A_g)}{d} \quad C_g = \frac{\kappa_g \epsilon_o A_g}{l} \quad (17)$$

The corresponding relation between the void fraction and the output signal of the capacitance sensor in the case of elongated bubble can be written as

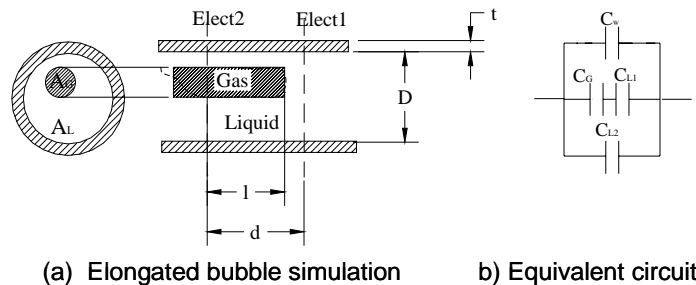


Fig. (6). a) Geometrical simulation of elongated bubble in ring type sensor. b) Equivalent capacitance circuit.

$$C_T = \frac{\epsilon_o}{d} \left[\frac{\pi D^2}{4} \left\{ \kappa_w \left(\left(1 + \frac{d}{t} \right) - 1 \right) + \kappa_L \left(1 - \frac{\alpha d}{l} \right) \right\} + \frac{l^2}{\alpha \kappa_s} + \frac{l^2 \left(\frac{d}{l} - 1 \right)}{\alpha \kappa_L} \right]$$

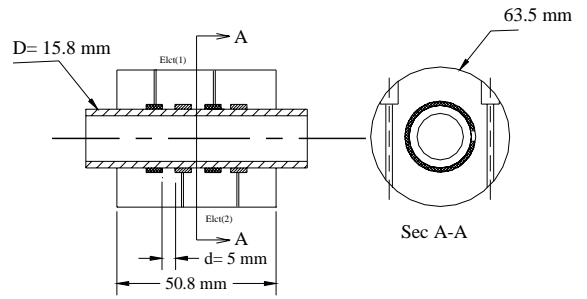
where $\frac{d}{l} > 1$.

The above analysis can be extended to different flow regimes, where the level of complexity of the analysis depends on the complexity of the flow regime and the required accuracy of the modelling.

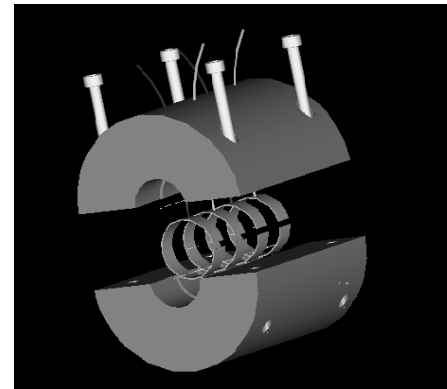
5. DESIGN AND CHARACTERIZATION OF THE SENSORS

Based on the theoretical analysis, ring and concave type sensors were designed and constructed for a tube having inside and outside diameter of 12.7 and 15.8 mm, respectively. The schematic diagrams with the basic dimensions of the sensors are shown in Figs. (7 & 8). The ring type sensor consists of two pairs of active electrodes made of 5 mm brass strips spaced 2 mm apart to increase the signal to noise ratio by amplifying the absolute value of the capacitance circuit. This geometry provides sufficient volumetric resolution to resolve the characteristics of the slug flow regimes. Two separate half hollow cylinders made of acrylic are used for housing the electrodes as show in Fig. (7a & b), and the unit is shielded using a 0.5 mm thick grounded brass electrode to eliminate stray capacitance between any of the electrodes, circuit and the wires. The housing is sandwiched together over the test section pipe and fastened using acrylic screws to make sure the electrodes are firmly in contact with the tube surface. The noise on the signal due to the surroundings and orientation of the connection wires was eliminated in the present design by increasing the separation distance between the electrodes and the shield relative to the separation distance between electrodes as suggested by Elkow and Rezkallah [23]. The length of the electrode for the concave type sensor is taken as 10 mm, and both electrodes are equal in length to decrease the nonlinearity in the sensor response as recommended by Elkow and Rezkallah [23]. Two pairs of electrodes were used with spacing of 6 mm to have the same spatial resolution as the ring type for comparison. In the experimental work reported here, the distance between the electrodes and the shielding was experimentally optimized to reduce the noise due to ground current and electric field leakage. The output capacitance from the sensors is measured using a Boonton 72B capacitance meter operated at an excitation frequency of 1 MHz. The accuracy of the meter is $\pm 4\%$ in the 10 pF range with meter resolution of at least 0.001 of the range. The analog output voltage signal from the capacitance meter is sampled using a 16-bit A/D converter at a sampling rate up to 2 KHz.

The sensors were calibrated over the full range of void fractions to verify the theoretical design approach. A static calibration was performed using simulated stratified and annular flow patterns, and a dynamic *in situ* calibration was performed to investigate the effect of the noise from the surroundings such as from other operating devices on the output signal of the sensors. It should be noted that the effect



a) Schematic of the ring type capacitance sensor.



b) Solid model.

Fig. (7). Ring type capacitance sensor.

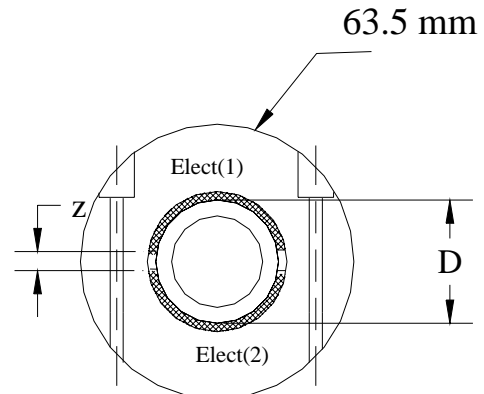


Fig. (8). Geometrical simplification of the concave type capacitance sensor.

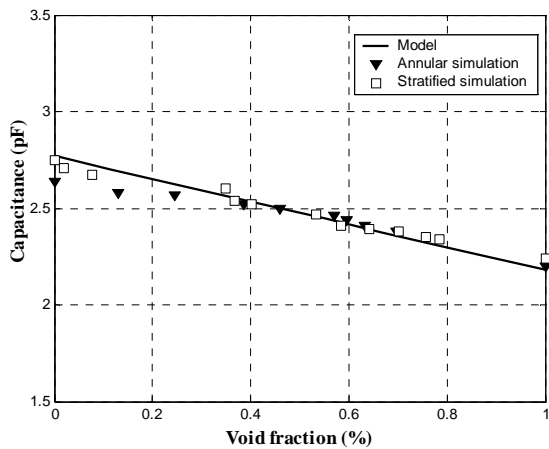
of the operating temperature was taken into consideration in the calibration tests. The calibration tests were used to compare the performance of the two types of sensors based on better sensitivity for the same spatial resolution as described in details by Ahmed [31].

5.1. Sensor Calibration

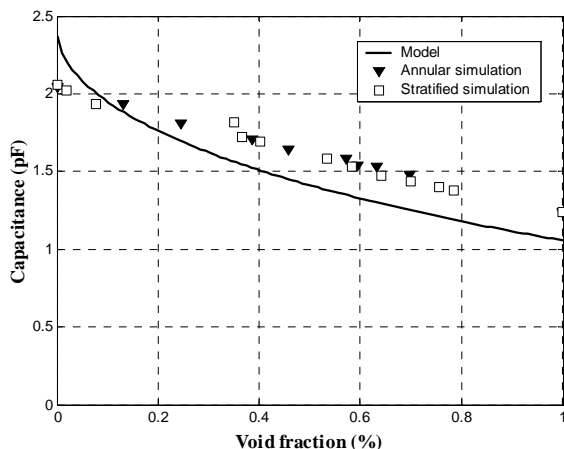
Canvas based Phenolic rods with the same dielectric constant as oil ($\kappa=5.45$) are used to represent the liquid in the static calibration at ambient temperature. The solid rods with

a diameter equal to the inside pipe diameter of the test section (12.7 mm) are machined to mimic different flow regimes. The lengths of these pieces are the same and equal to 13 cm. Calibration was carried out for two different flow patterns, namely annular and stratified flow. To represent annular flow, holes of different diameter were drilled through the center of each piece. Nine pieces were generated to simulate different void fractions. For stratified flow, eleven separate sections were milled off the rod. The value of void fraction for each piece can be calculated using the geometry.

A comparison between the results from the theoretical models and the experimental data for the off-line calibration is presented in Figs. (9a & b) for both ring and concave sensors. The experimental results show that the relation between the capacitance and void fraction for both types of sensors is approximately linear. The deviation between the model and experimental results is due to the assumption of



a) Static calibration for ring type capacitance sensor.



(b) Static calibration for concave type capacitance sensor.

Fig. (9). Static calibration for capacitance sensors.

perfect shielding and also due to a non-uniform electrical field between the electrodes, with the discrepancy being higher for the concave type sensor. This is because the assumption of a constant electric field between the electrodes is more applicable for the ring type sensor than for the concave type. The non-linearity of the model results for the concave type sensor is due to the electrical circuit analogy which gives rise to a series capacitance circuit, where the total capacitance is a non-linear function of the individual capacitances. For the ring type sensors, the total capacitance between the electrodes is a summation of capacitances in parallel. The calibration data showed a correlation coefficient of 0.928 and a precision error of 0.04 with 95% confidence level for the ring type sensor, while the agreement between the experiments and the theory for the concave sensor was within 18%.

Measurements were performed with the sensors installed on the air-oil two phase flow loop which discussed in details by Ahmed [32]. The density and viscosity of the oil used are 973.05 kg/m^3 and 0.026 Pa.s , respectively. The air and oil are then mixed through an annular mixer. The oil flows on the outside of an inner perforated pipe, while the air flows in the inner pipe and enters the oil stream through 380 0.79-mm diameter perforations. The air-oil mixture passes through the horizontal test section, which has a total length of 3.5 m.

Tests were performed with single phase oil ($\alpha=0$) and single phase air ($\alpha=1$) to check the range of the output signal of the sensors. A number of tests were performed for stratified flow by adjusting the depth of the oil in the pipe to check the linearity of the capacitance-void fraction relation. Results show that the sensitivity is the same for both the *in situ* and static calibrations, however, the absolute values of the capacitances at zero and 100% void for the two cases are off by 5 to 10%. Therefore, the calibration curves were checked against the dynamic results before the experimental data were taken. Repeatability tests were also performed and the results indicated that the variation in void fraction is between 2% to 3.5%.

The capacitance measurements in the air-oil flow tests are in the range 0.1 to 15 pF , and proper shielding against stray capacitance is required to obtain a good signal to noise ratio (SNR). The range of the noise frequencies due to the equipment and electrical devices near the test rig were determined using a frequency analyzer and was found to be lower than 100Hz in this case. The electronic circuit was modified to eliminate the environment noise using a high pass filter.

The void fraction can be related to the normalized capacitance (C_n) defined as:

$$C_n = \frac{C_{\text{all-oil}} - C_{\text{measured}}}{\alpha_{\text{all-oil}} - \alpha_{\text{all-air}}} \quad (18)$$

The correlation between the void fraction and normalized capacitance is found by applying a linear regression to the calibration data for the ring type sensor and is given by,

$$\alpha = 0.756 \cdot C_n \quad (19)$$

with a correlation coefficient of 0.95.

5.2. Time Constant

The definition of the time constant of the capacitance sensor here is referred to the time interval required for the sensor-meter to change 70% from one state or condition to another. The time constant for both types of capacitance sensors was obtained experimentally by applying a unit step signal and recording the sensor response Fig. (10). The time constant for both types of capacitance sensors using equation (20) is found to be approximately 40 μs, corresponding to a dynamic response of 25 kHz. Fast Fourier transform analysis of the current flow fluctuations in the present study showed that the major fluctuations in the void fraction were below 1 kHz, thus the response of the sensors is more than adequate

$$\frac{Y_t - Y_{\text{initial}}}{Y_{\text{max}} - Y_{\text{initial}}} = 1 - e^{-t/\tau} \tag{20}$$

5.3. Sensitivity

The sensitivity of the sensor can be defined as:

$$\text{Sensitivity} = \frac{C_{\text{all-liquid}} - C_{\text{all-air}}}{\alpha_{\text{all-liquid}} - \alpha_{\text{all-air}}} = C_{\text{all-liquid}} - C_{\text{all-air}} \tag{21}$$

and needs to be maximized. The sensitivity depends on the geometrical shape and gap between the electrodes, which also affects the spatial resolution of the sensor. The effect of the design parameters such as the electrode width and spacing were studied using equations (11) and (12) for both sensors. For the ring type sensor, the main dimension that affects the sensitivity is the spacing between the electrodes (d). The results show that the sensitivity increases as the spacing decreases Fig. (11), which also results in a better spatial resolution, with the only limitation being in the fabrication of the sensor. For the concave sensor, the sensitivity increases as the electrode separation (z) decreases Fig. (12a), and the electrode length leads to a poor spatial resolution as shown in Fig. (12b). In general, the sensitivity of the ring type sensor is found to be higher than the concave type for the same spatial resolution. The sensitivity of the ring sensor was found to be approximately 0.75 pF, while for the concave sensor it was 0.6 pF.

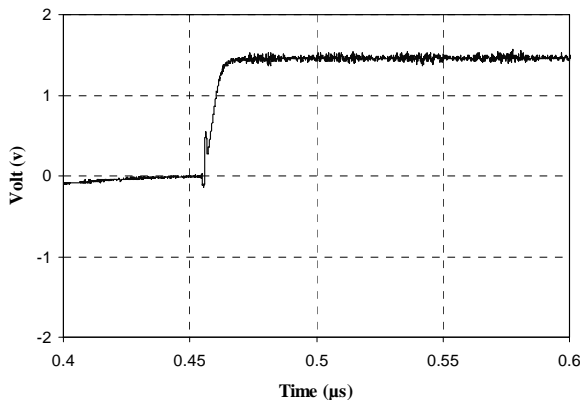


Fig. (10). Capacitance Sensor response to an input step function.

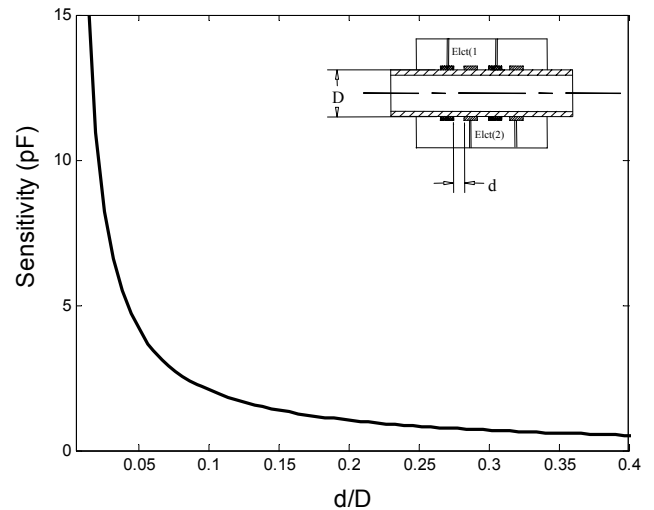
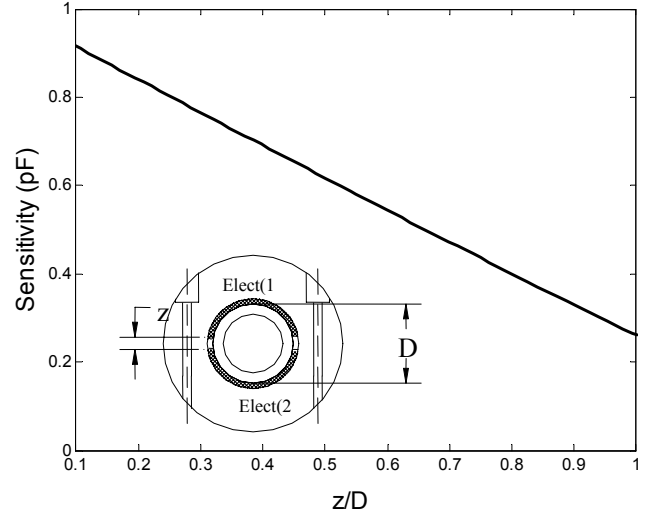
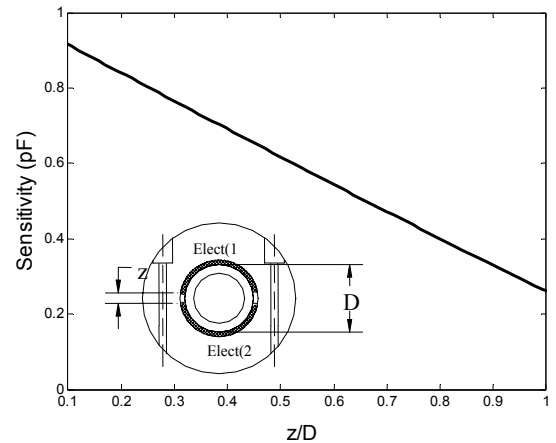


Fig. (11). Effect of electrode spacing on the sensitivity of ring type sensor.



(a) Effect of electrode separation.



(b) Effect of electrode length.

Fig. (12). The effect of sensor dimensions on the sensitivity for concave type sensor.

The effect of the flow regime on the sensitivity of the capacitance sensor can be estimated. For example, in the case of elongated bubbles, the sensitivity can be calculated using equation (18) along with equation (21). The sensitivity as a function of void fraction for different bubble length to electrode spacing length ratios for an electrode spacing of 10 mm is shown in Fig. (13). It should be noted that the sensitivity is also affected by the electrode spacing and for the ring type sensor an electrode spacing of less than 2 mm is required for a high sensitivity. For this electrode spacing, the effect of (l/X) is found to be neglected, which means that the sensor gives an approximate volumetric void fraction equal to the cross sectional value for bubbly flow.

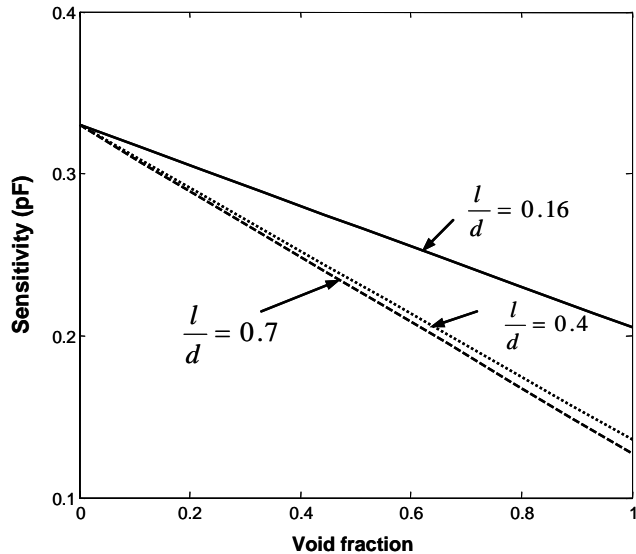


Fig. (13). The sensitivity of ring type sensor in case of elongated bubble flow.

5.4. Measurement Uncertainty

The total flow rate through the test section was maintained within $\pm 2\%$ of the average value while the void fraction measurements were taken. The main source of uncertainty in the void fraction measurement was the noise in the sensor signal from the surrounding equipment such as the oil pump and the biases of the voltage signal, sensor spacing and position. This uncertainty was calculated to be in the range of $\pm 6\%$ over the entire range of void fraction.

6. FLOW PATTERN IDENTIFICATION

Flow pattern identification can be performed either by visual inspection of the flow in a transparent pipe or by measuring and quantifying the fluctuations of the flow parameters such as void fraction (Jones and Zuber [30]) or dynamic pressure (Keska and Williams [33]), which reflect the flow structure. The flow pattern recognition from the signal fluctuations can be done by analyzing the probability density function (PDF) or power spectral density function (PSD) of the time trace signal [30]. In the present study, the applicability of the capacitance sensors for flow pattern identification was investigated. Only the ring type sensor is considered here since it has a better sensitivity than the concave type for the same spatial resolution. The time averaged void fraction and the probability density function

(PDF) of the void fraction signal is used in this instance to identify the flow pattern. The flow regimes are also obtained using a high speed camera for validation. Three main flow regimes and their corresponding PDF distributions are discussed here for two-phase air-oil through a horizontal pipe. These three basic flow regimes are: elongated bubble, slug and annular flow. All the data presented was collected at 2 kHz over a period of 50 sec.

Figures (14a,b & c) illustrate the time trace, PDF and void fraction signal respectively for a typical slug flow while an image of the corresponding flow pattern using the high speed video system is presented in Fig. (14d). The time trace is characterized by an intermittent void fraction signal that fluctuates between a high and low value. The high void fraction ($a=0.29$) correspond to the passage of a long gas bubble, while the low void fraction indicates the passage of the liquid slug. Small bubbles in the tail of the long bubbles gives rise to the low void fraction ($a=0.04$). Although the capacitance sensor measures the volumetric void fraction over a tube length of 1.65 D, the sensor seems to be sensitive to bubbles that are entrained in the liquid slugs as can be seen in the time trace signal. In order to distinguish between two signals having double peaks on the PDF diagram, the power spectral density (PSD) was used. In this case, additional information about the flow structure was obtained such as the bubble and liquid slug frequencies. The power spectral density (PSD) for the slug flow signal shown in Fig. (14c) is characterized by two dominant frequencies, corresponding to the liquid slug and the gas bubble frequencies. In Fig. (14c), the slug frequency is approximately 118 Hz, while the frequency of the small bubbles is 228 Hz. For elongated bubble and slug flows, a double peak PDF is obtained, one at low void fraction corresponding to the liquid slugs and the other at high void fraction due to the gas slugs. The time trace and PSD in this case are used to distinguish between the two cases. For elongated bubbly flow, the void peaks on the time trace signal occur at a higher frequency than for slug flow (Fig. (15a) through d). This is indicated in the power spectral density (PSD) of the signal where a higher frequency of 394 Hz is obtained for the case of elongated bubble flow Fig. (15c), while a frequency of 228 Hz is obtained for the case of slug flow Fig. (14c).

The PDF for annular flow is characterized with a single peak at high void fraction as shown in Fig. (16b), while the time trace shows small oscillations around a high mean value of void fraction ($a=0.54$) indicating the unsteady surface waves of the liquid film. It should be noted that, as the peak in the PDF becomes narrower, the liquid film thickness becomes more nearly constant.

7. CURRENT & FUTURE DEVELOPMENTS

Electrical capacitance is an innovative technique for measurement of two-phase flows. In this paper, a review including most recent patents developed for two-phase flow measurements using capacitance-based sensor was presented. Also, in this work, a novel systematic method for the design of capacitance sensors for void fraction measurement and flow pattern identification was developed and discussed in detail. Two types of capacitance sensors, ring and concave type, have been analyzed. The phase or void distribution is represented by an equivalent capacitance circuit to estimate

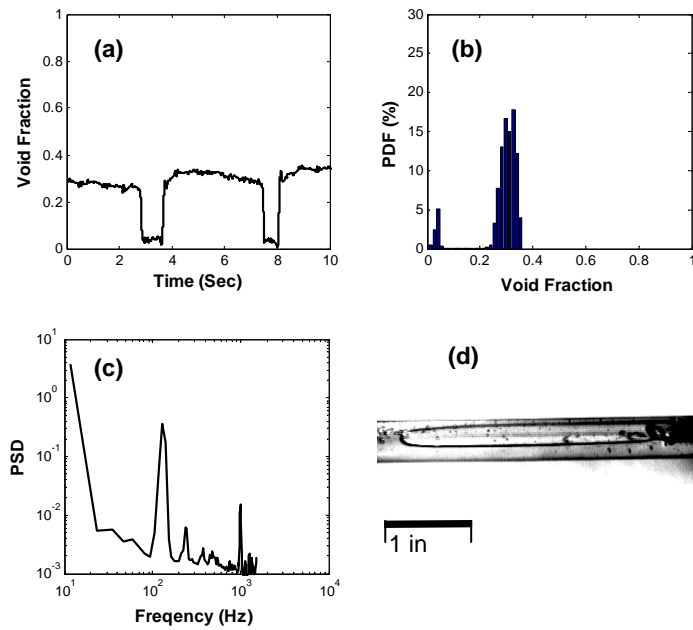


Fig. (14). (a) Time trace signal, (b) PDF, (c) PSD and (d) Flow image for intermittent (slug) flow regime ($G_{L1} = 605 \text{ kg/m}^2 \cdot \text{s}$ and $x=0.0077$).

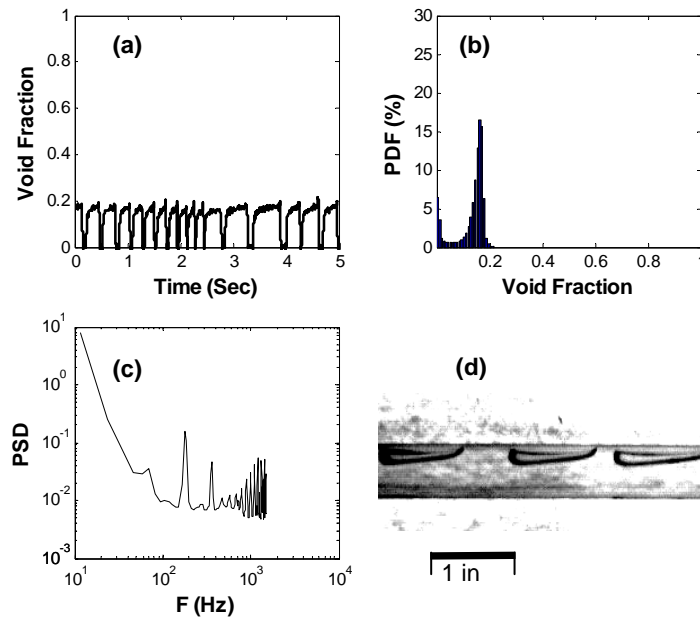


Fig. (15). (a) Time trace signal, (b) PDF, (c) PSD and (d) Flow image for elongated bubble flow regime ($G_{L1} = 790 \text{ kg/m}^2 \cdot \text{s}$ and $x=0.001$).

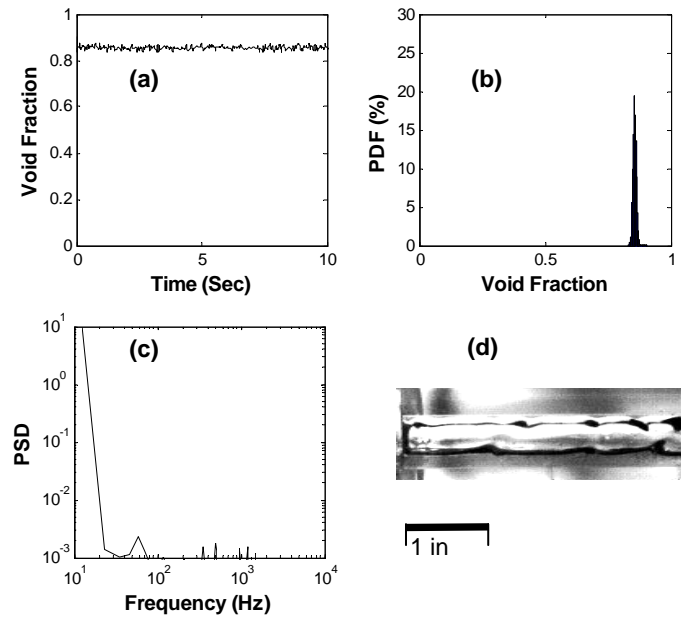


Fig. (16). (a) Time trace signal, (b) PDF, (c) PSD and (d) Flow image for annular flow regime ($G_{LI} = 395 \text{ kg/m}^2 \cdot \text{s}$ and $x=0.15$).

the sensitivity of both concave and ring type sensors. The sensitivity of the ring type sensor increases as the separation distance between the electrodes decreases, which also increases the spatial resolution of the sensor. The sensitivity of the ring type sensor is found to be higher than the concave type for the same spatial resolution. Both types of sensors were fabricated and tested in an air-oil flow loop. The void fraction predictions from the theoretical models for the sensor design are within 15% of the experimental data. Calibration of the sensors shows that the output capacitance is linearly related to the void fraction for both types of sensors. The volumetric average void fraction is independent of the flow pattern for both ring type and concave type sensors, which is useful to obtain accurate measurements of average void fraction. The capacitance sensors are very sensitive to flow regime change and can be used to identify the flow pattern. The mean value and the probability density function of the instantaneous void fraction signal is used to identify the flow regime. Both the slug and elongated bubble flow patterns are characterized by a double peak PDF with one peak at a high void fraction and one at a low void fraction. However, the time trace signal and the power spectral density (PSD) can be used to distinguish between the two flow regimes. The time trace signal shows that, for elongated bubble the fluctuations occur at a higher frequency than for slug flow, which is reflected in the power spectral density (PSD). A single sharp peak in the PDF at high void fraction characterizes the annular flow pattern.

NOTATION

A	=	Area
D	=	Diameter (mm)
E	=	Electric field
α	=	Void fraction

l	=	Electrode length (mm)
t	=	Pipe wall thickness (mm)
T	=	Time (sec)
V	=	Potential difference (volt)
τ	=	Time constant (sec)
κ	=	Dielectric constant

SUBSCRIPT

o	=	Refer to free space
c	=	Charge
P	=	Polarization charge
L	=	Liquid
G	=	Gas
T	=	Total
w	=	wall

REFERENCES

- [1] Lowe DC, Rezkallah KS. A capacitance sensor for the characterization of microgravity two-phase liquid-gas flows. *Meas Sci Technol* 1999; 10: 965-975.
- [2] Boothroyd RG. *Flowing gas-solids suspensions*. Chapman & Hall, London, 1971.
- [3] Green RG, Thorn R. Sensor systems for lightly loaded pneumatic conveyors. *Powder Technol* 1998; 95: 79-92.
- [4] Jaworski AJ, Dyakowski T. Application of electrical capacitance tomography for measurement of gas-solids flow characteristics in a pneumatic conveying system. *Measurment Sci Technol* 2001; 12: 1109-1119.
- [5] Ostrowski K, Luke SP, Bennett MA, Williams RA. Real-time visualization and analysis of dense phase powder conveying. *Powder Technol* 1999; 102: 1-13.
- [6] Sen S, Das PK, Dutta PK, Maity B, Chaudhuri S, Mandal C, Roy SK. Pc-based gas-solids two-phase mass flow meter for

- pneumatically conveying systems. *Flow Measurment Instrument* 2000; 11: 205-212.
- [7] Harvel GD, JS. Chang. Electrostatic multiphase flow measurement techniques. *Handbook of Electrostatic Processes* ch.13 J. S. Chang, A. J. Kelly, and J. M. Crowley, eds. Marcel Dekker, Inc., New York, 1995.
- [8] Barratt IR, Yan Y, Byrne B, Bradley MSA. Mass flow measurement of pneumatically conveyed solids using radiometric sensors. *Flow Measurment Instrument* 2000; 11: 223-235.
- [9] Morse TD, Bellou CD. The uniformity of fluidization, its measurements and use. *Chem Engng Prog* 1951; 47: 199-211.
- [10] Lanneau KP. Gas-solid contacting in fluidized beds. *Trans Instn Chem Engrs* 1960; 38: 125-143.
- [11] Chang JS, Girard R, Raman R, Tran EBP. Measurement of void fraction in vertical gas-liquid two-phase flow by ring type capacitance transducer. *Mass flow Measurements*. ASME Press, New York, 1984.
- [12] Tortora PR, Ceccio SL, Trujillo SM, O'Hern TJ, Shollenberger KA. Capacitance measurements of solid concentration in gas-solid flows. *Powder Technol* 2004; 148: 92-101.
- [13] Dyakowski T, Edwards RB, Xie CG, Williams RA. Application of capacitance tomography to gas-solid flows. *Chem Eng Sci* 1997; 52(13): 2099-2110.
- [14] Dyakowski T, Jeanmeure LFC, Jaworski AJ. Applications of electrical tomography for gas-solids and liquid-solids - a review. *Powder Technol* 2000; 112: 174-192.
- [15] Brown GJ, Reilly D, Mills D. Development of an ultrasonic tomography system for application in pneumatic conveying. *Meas Sci Technol* 1996; 7: 396-405.
- [16] Steiner G, Wegleiter H, Watzenig DA. A dual-mode ultrasound and electrical capacitance process tomography sensor. *IEEE Sensors*, Irvine, CA, USA, page Cat. No. 05CH37665C, 2005.
- [17] Jiang T, Xiong Y. Measurement of the velocity and mass flow rate in gas-solid flow with electrostatic method. *J Huazhong Univ Sci Tech* 2005; 33 (1): 93-95.
- [18] Andrade, T.L.: US2007134042 (2007).
- [19] Huang SM, Plaskowski AB, Xie CG, Beck MS. Tomographic imaging of two-component flow using capacitance sensors. *J Phys E Sci Instrum* 1989; 22: 173-177.
- [20] Merilo M, Dechene RL, Cicowlas WM. Void fraction measurement with a rotating electric field conductance gauge. *J Heat Transfer Trans ASME* 1977; 99: 330-331.
- [21] Lucas GP, Simonian S. Towards a phase-distribution-independent impedance volume-fraction meter. *Flow Measurment Instrument* 1991; 2: 105-114.
- [22] Geraets JJM, Borst JC. A capacitance sensor for two-phase void fraction and flow pattern identification. *Int J Multiphase Flow* 1988; 14: 305.
- [23] Elkow KJ, Rezkallah KS. Void fraction measurement in gas-liquid using capacitance sensors. *Meas Sci Technol* 1996; 7: 1153.
- [24] Gamio JC, Castro J, Rivera L, Alamilla J, Garcia-Nocetti F, Aguilar L. Visualisation of gas-oil two-phase flows in pressurized pipes using electrical capacitance tomography. *Flow Measurment Instrument* 2005; 16: 129-134.
- [25] Wang, M.C.: US2007570054 (2007).
- [26] Kendoush AA, Sarkis ZA. Improving the accuracy of the capacitance method for void fraction measurement. *Exp Thermal and Fluid Sci* 1995; 11: 321.
- [27] Hammer EA, Tollefsen J, Olsvik K. Capacitance transducers for non-intrusive measurement of water in crude oil. *Flow Measurment Instrument* 1989; 1: 51-58.
- [28] Heerens WC. Application of capacitance techniques in sensor design (review article). *J Phys E Sci Instrum* 1986; 19: 897-906.
- [29] Atsushi, K.C.: US2007/0103171A1 (2007).
- [30] Jones OC, Zuber N. The interrelation between void fraction fluctuations and flow pattern in two-phase flow. *Int J Multiphase Flow* 1975; 2: 273.
- [31] Ahmed WH. Capacitance sensors for void fraction measurements and flow pattern identification in air-oil two-phase flow. *IEEE Sensors J* 2006; 6(5): 1153-1163.
- [32] Ahmed WH, Ching CY, Shoukri M. Characteristics of air-oil two-phase flow across a sudden expansion. In *Proc. 4th ASME/JSME Joint Fluid Eng Conf* volume 2B, 1765: 1772, Honolulu, HI, USA, July 6-10, 2003.
- [33] Keska JK, Williams BE. Experimental comparison of flow pattern detection techniques for air-water mixture flow. *Exp Thermal & Fluid Sci* 1999; 19: 1-12.